Time-resolved fluorescence studies of tryptophan mutants of Escherichia coli glutamine synthetase: Conformational analysis of intermediates and transition-state complexes

ARTICLE *in* PROTEIN SCIENCE · MARCH 2008

Impact Factor: 2.85 · DOI: 10.1002/pro.5560010306 · Source: PubMed

2 AUTHORS, INCLUDING:

William M Atkins
University of Washington Seattle
135 PUBLICATIONS **3,243** CITATIONS

Protein Science (1992), *1*, 342–355. Cambridge University Press. Printed in the USA.

Time-resolved fluorescence studies of tryptophan mutants of *Escherichia coli* glutamine synthetase: Conformational analysis of intermediates and transition-state complexes

WILLIAM M. ATKINS AND JOSEPH J. VILLAFRANCA
Department of Chemistry, The Pennsylvania State University, University Park, Pennsylvania 16802
(RECEIVED July 30, 1991; ACCEPTED October 11, 1991)

Abstract

Single tryptophan-containing mutants of low adenylylation state *Escherichia coli* glutamine synthetase have been studied by frequency-domain fluorescence spectroscopy in the presence of various substrates and inhibitors. At pH 6.5, the Mn-bound wild-type enzyme (wild type has two tryptophans/subunit) and the mutant enzymes exhibit heterogeneous fluorescence decay kinetics; the individual tryptophans are adequately described by a triple exponential decay scheme. The recovered lifetime values are 5.9 ns, 2.6 ns, and 0.4 ns for Trp-57 and 5.8 ns, 2.3 ns, and 0.4 ns for Trp-158. These values are nearly identical to the previously reported results at pH 7.5 (Atkins, W.M., Stayton, P.S., & Villafranca, J.J., 1991, *Biochemistry 30*, 3406–3416). In addition, Trp-57 and Trp-158 both exhibit an ATP-induced increase in the relative fraction of the long lifetime component, whereas only Trp-57 is affected by this ligand at pH 7.5. The transition-state analogue L-methionine-(R,S)-sulfoximine (MSOX) causes a dramatic increase in the fractional intensity of the long lifetime component of Trp-158. This ligand has no effect on the W158S mutant protein and causes a small increase in the fractional intensity of the long lifetime component of the W158F mutant protein. Addition of glutamate to the ATP complex, which affords the γ-glutamylphosphate–ADP complex, results in the presence of new lifetime components at 7, 3.2, and 0.5 ns for Trp-158, but has no effect on Trp-57. Similar results were obtained when ATP was added to the MSOX complex; Trp-57 exhibits heterogeneous fluorescence decay with lifetimes of 7, 3.5, and 0.8 ns. Decay kinetics of Trp-158 are best fit to a nearly homogeneous decay with a lifetime of 5.5 ns in the MSOX–ATP inactivated complex. These results provide a model for the sequence of structural and dynamic changes that take place at the Trp-57 loop and the central loop (Trp-158) during several intermediate stages of catalysis.

Keywords: *Escherichia coli*; fluorescence studies; glutamine synthetase; transition-state complexes; tryptophan mutants

Glutamine synthetase (GS) plays a central role in the nitrogen metabolism of both prokaryotes and eukaryotes, catalyzing the ATP-dependent condensation of glutamate with ammonia to form glutamine (Ginsburg, 1972; Stadtman & Ginsburg, 1974). The bacterial enzymes consist of a highly symmetrical dodecamer formed by two face-to-face hexameric rings. The high-resolution X-ray crystal structure of the enzyme from *Salmonella typhimurium* provides a valuable model for understanding structure–function relationships of these enzymes (Almassy et al., 1986; Yamashita et al., 1988). Notably, the 12 active sites found in the aggregate protein lie between the N-terminus of each subunit and the C-terminus of an adjacent subunit. Two domains of GS that have been proposed to be functionally important are the Trp-57 loop and the central loop (Kinemage 1; Almassy et al., 1986; Yamashita et al., 1988). Each of these domains contains a single tryptophan residue, and these are the only two tryptophans found in the *Escherichia coli* protein (Colombo & Villafranca, 1986). In order to understand structural and

Reprint requests to: Joseph J. Villafranca, Department of Chemistry, The Pennsylvania State University, University Park, Pennsylvania 16802.

Abbreviations: W57L, the site-directed mutant that has Trp-57 replaced by leucine; W158S or W158F, the site-directed mutants that have Trp-158 replaced by serine or phenylalanine; glutamylphosphate–ADP–GS, the ternary complex formed after the addition of ATP and glutamate to glutamine synthetase.

dynamic changes associated with function, we have used single tryptophan-containing mutants to determine the fluorescence decay kinetics of these individual tryptophan residues.

The Trp-57 loop lies at the outer diameter of the ring structure and connects two β-strands that traverse the active site. In the substrate-free crystal structure, the Trp-57 loop is exposed to solvent and lies within a few angstroms of the site of adenylylation of the adjacent subunit (Kinemage 2). Many prokaryotic GS enzymes are regulated in a complex fashion by this type of covalent modification as well as by allosteric effectors. Specifically, a tyrosine residue is adenylylated to result in the down regulation of the Mg-bound form of GS from some organisms. This site is Tyr-397 for the *E. coli* enzyme. It has been proposed that specific interactions between the adenylyl group and the Trp-57 loop are necessary for this regulatory function (Almassy et al., 1986). The central loop, which contains Trp-158, lies across the active site from Trp-57, at the inner diameter of the dodecameric ring (Kinemage 3). This loop projects into the center of the ring structure and has been proposed to be involved in ligand-dependent conformational changes that alter the susceptibility of the central loop to proteolytic degradation in vitro (Dantry-Varsat et al., 1979). Furthermore, it has been reported that the central loop may be ADP-ribosylated, providing an additional means of covalent regulation (Moss et al., 1988).

We have recently reported results obtained with multifrequency phase/modulation fluorescence spectroscopy and site-directed mutants of *E. coli* GS, which contain individual tryptophan residues in either the Trp-57 loop or in the central loop (Atkins et al., 1991). Although other techniques have demonstrated ligand-induced global changes in the physical nature of GS (Maurizi & Ginsburg, 1982; Shrake et al., 1989), the combination of site-directed mutagenesis with time-resolved fluorescence provides details concerning local peptide dynamics within the Trp-57 loop and the central loop. This approach allows for the study of the conformational dynamics of each of these regions of the protein and the structural changes that accompany ligand binding. Time-resolved fluorescence spectroscopy has now been used to study the conformational heterogeneity of individual tryptophans in several proteins (Beechem et al., 1983; Eftnik & Wasylewski, 1989). Both tryptophans of *E. coli* GS demonstrate apparent conformational heterogeneity, characterized by multiexponential fluorescent decay kinetics. Addition of the substrate ATP causes a redistribution of the microconformations of Trp-57, which becomes less solvent exposed and less heterogeneous in the presence of this ligand.

Here we focus on the other ligand-bound states of the protein. Binding of the transition-state analogue L-methionine-(R,S)-sulfoximine (MSOX) (Manning et al., 1969; Eads et al., 1988), and formation of the γ-glutamylphosphate–ADP or the MSOX-P–ADP complex results in conformational changes that are largely localized to the central loop. In addition, it is demonstrated that there is a pH-dependent change in the fluorescent parameters of Trp-158 associated with ATP binding, which may suggest a structural basis for the pH activity profile of the Mn-bound enzyme (Ginsburg et al., 1970; Ginsburg, 1972). With the previous results concerning the Trp-57 loop, the results presented here provide a model for the sequence of structural changes of these domains that are associated with various substrate-bound states of the protein.

Results

During the characterization of ligand-dependent changes in the fluorescent parameters of wild-type and mutant GS it became clear that the magnitudes of these effects are sensitive to pH. Previously we studied ATP binding at pH 7.4, which is close to the pH at which the crystals used for the X-ray structure were obtained (Janson et al., 1984). It is well documented, however, that the pH optimum for the biosynthetic reaction of the Mn-enzyme is near pH 6.5, with diminished activity at pH 7.5 (Ginsburg et al., 1970; Ginsburg, 1972). This pH profile is inverted relative to the Mg-enzyme, which has its greatest activity at pH 7.5. Therefore, we have designed experiments to study the effects of ligand binding on the tryptophan fluorescence of Mn-GS at pH values near 6.5 as well. Throughout the analysis we have ascribed individual fluorescent lifetime components to distinct microconformations of tryptophan residues, as many others have (Eftnik & Wasylewski, 1989; Hutnik & Szabo, 1989a,b; Royer et al., 1990). There has been considerable discussion concerning the source of heterogeneous decay in single-tryptophan-containing proteins (Lackowicz, 1983; Alcala et al., 1987; Beechem & Gratton, 1988). We see no indication of excited state reactions or other possible causes of heterogeneous decay.

Substrate-free GS at pH 6.5

It was first necessary to compare the lifetime distribution of the individual tryptophans at pH 6.5 to the results obtained at pH 7.4 (Atkins et al., 1991). The lifetime values and fractional intensities are nearly identical to those observed at the higher pH, and the results of global analysis for the data acquired at pH 6.5 are summarized in Table 1. Specifically, the fluorescence decay kinetics of the wild type, the W57L mutant, and the W158S mutant are best described by a sum of three discrete exponentials with recovered lifetime values near 5 ns, 2 ns, and <1 ns (Table 1). The minor differences observed at pH 6.5 compared to those observed previously at pH 7.4 may be partially attributable to instrumental variation.

Trp-57 (W158S) is characterized by a slightly larger fraction of the median, 2-ns, component compared to the

Table 1. *Global analysis for wild type, W158S, and W57L*[a]

Protein	χ^2	Lifetimes (ns)	Fraction intensity, 320, 330, 360, 380 nm
Wild type	0.44	4.84 +0.74/−0.21	0.49, 0.51, 0.56, 0.56
		1.99 +0.51/−0.20	0.47, 0.45, 0.42, 0.42
		0.27 +0.09/−0.11	0.04, 0.03, 0.02, 0.02
W57L	0.78	5.81 +1.1/−0.9	0.36, 0.38, 0.42, 0.47
		2.37 +0.64/−0.34	0.58, 0.56, 0.54, 0.49
		0.41 +0.22/−0.21	0.05, 0.06, 0.04, 0.04
W158S	1.20	5.92 +1.2/−0.16	0.36, 0.40, 0.46, 0.51
		2.68 +0.52/−0.23	0.58, 0.55, 0.48, 0.43
		0.54 +0.20/−0.17	0.08, 0.05, 0.06, 0.06

[a] Errors reported for individual lifetime values are the high and low limits of resolution at the 67% confidence level, as provided by Globals Unlimited. Measurements were made with 10 μM protein in 20 mM Hepes, pH 6.5, 100 mM KCl, 1 mM $MnCl_2$, at 20 °C. Slit widths were 2 mm. Modulation frequencies of 2, 6, 8, 16, 28, 44, 72, 104, and 110 MHz were used.

distribution observed at pH 7.4. This appears to be a direct result of the change in pH, as determination of the phase angles and modulation ratios at pH 7.3 with the same band-pass filters affords identical lifetime values with a shift in fractional contribution toward the longer lifetime component, as was observed previously (Atkins et al., 1991). At the lower pH there is as much as 60% of the median lifetime component for Trp-57, whereas at pH 7.4 this component provides only 35–45% of the total fractional intensity. Thus, there appears to be a small pH effect on the fractional contribution of the lifetimes associated with Trp-57. It is particularly striking that at pH 6.5, both tryptophans are described by a triple exponential decay with a preponderance of the median and long lifetime components, as was observed at pH 7.4. Thus, the relative distribution of the lifetime components of Trp-57 may change slightly as a function of pH, but there do not appear to be any major structural rearrangements in the environment of either tryptophan, resulting in the recovery of new lifetime values. Attempts to fit the phase and modulation data to the sum of two discrete exponentials or to a single exponential resulted in χ^2 values of 9 or greater. This is very similar to the results reported earlier so all of the analysis is not included here. Also, the χ^2 values were raised significantly when the data were fit to unimodal or trimodal continuous Lorentzian distribution models. Again, this is directly analogous to the results observed at pH 7.4. Furthermore, time-domain experiments afford essentially identical results (not shown), so it is clear that at both pHs each of the individual tryptophans requires the sum of at least three exponential decays to adequately fit the data.

ATP binding

We have previously described the effects of ATP on the fluorescence lifetime distribution of Trp-57 at pH 7.4 (Atkins et al., 1991). At pH 6.5 a nearly identical result is observed. Specifically, there is a dramatic shift toward lower frequencies in the phase and modulation data when ATP binds to the W158S mutant. Global analysis indicates that this effect is most consistent with a model in which the lifetime components redistribute such that the 5-ns component, which is 49–60% of the fractional intensity in the absence of ATP, becomes 90% of the fractional intensity when ATP is added. Although it is possible that new lifetime components are obtained in the presence of ATP, global analysis indicates that within the resolution of the data (<1 ns) there is simply a redistribution of microconformational states that retain the same lifetime values. Because this has been described in detail in the previous work, the global analysis and phase and modulation data are not included here. Similarly, the wild-type enzyme demonstrates an effect of ATP binding at pH 6.5 that is nearly identical to the results described elsewhere (Atkins et al., 1991).

In contrast, the effect of ATP on Trp-158 at pH 6.5 is slightly different from that observed at pH 7.4. At the higher pH very little perturbation of the Trp-158 is observed, whereas at pH 6.5 it becomes apparent that this tryptophan demonstrates a small shift to lower modulation frequencies in the phase and modulation data. Global analysis indicates that no new lifetime components are recovered as a result of ATP addition, but instead the existing lifetime components change in their fractional intensities. When the individual lifetime components are constrained to remain the same for the different ligand states (±ATP), the recovered lifetime values are essentially identical to those recovered in the independent analysis of the W57L mutant in the absence of ATP (5.84 ns, 2.38 ns, and 0.51 ns). The χ^2 value for this linkage scheme is 1.82. The fractional intensities change from 29 to 40% of the long lifetime and 55 to 63% of the median lifetime in the absence of ATP and from 67 to 72% of the long lifetime and 26 to 29% of the median lifetime in the presence of ATP. This is similar to the effects observed with Trp-57 (W158S), although the effect is less pronounced. For Trp-57, the long lifetime component is driven to 90% of the total fractional intensity when ATP is present. It appears, therefore, that like Trp-57, Trp-158 undergoes a small redistribution of existing microconformational states when ATP binds. It is possible that the observed pH activity profile is correlated to the pH dependence of the structural change at Trp-158

accompanying ATP binding. In fact, it has been reported that the binding affinity of ATP for the Mn-enzyme varies with pH and increases as the pH decreases from 7.5 to 6.0 (Denton & Ginsburg, 1969).

In order to further characterize this pH dependence, the relative quantum yields of the individual tryptophans of *E. coli* GS were determined at several pHs in the presence and absence of ATP. These have been determined from the total integrated emission intensities between 315 and 450 nm, which have been normalized to the individual optical densities (ODs) at 295 nm for each sample as described in the Materials and methods. As can be seen in Figure 1, there is little variation in the quantum yield of either tryptophan as a function of pH in the absence of ligand. Trp-57 has a significantly higher quantum yield, 2.5-fold, as mentioned previously (McNemar et al., 1991). With ATP bound, Trp-158 shows a dramatic two-fold increase in quantum yield as the pH decreases from 7.5 to 6.5. Although Trp-57 contributes two to three times as much intensity in the absence of ligands at pH 7.4, at the lower pHs Trp-158 contributes nearly as much emission to the ATP complex.

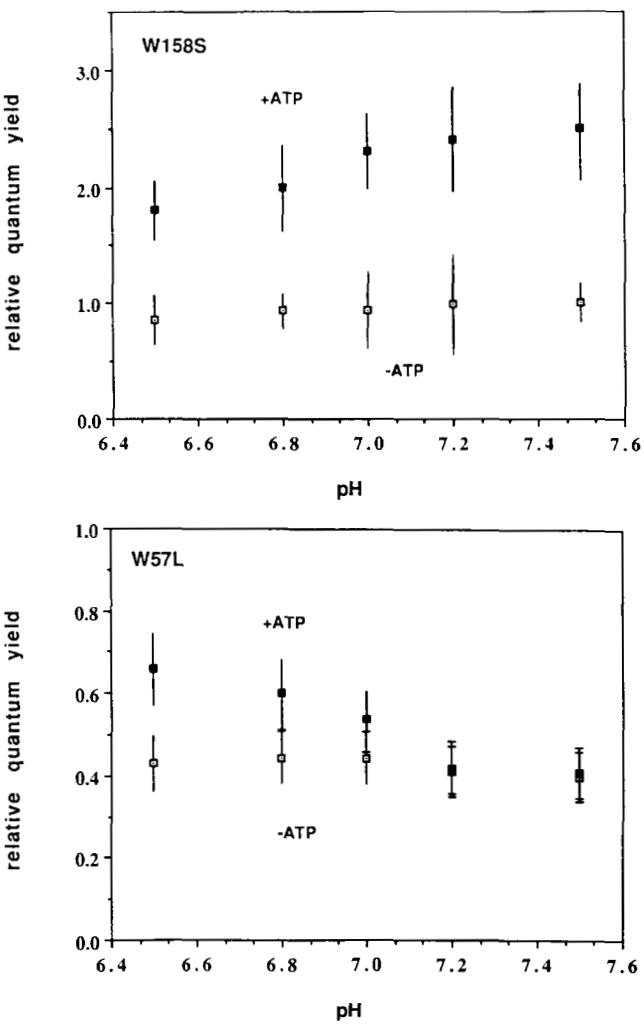

Fig. 1. Relative quantum yields of Trp-57 and Trp-158 as a function of pH. The relative quantum yields have been normalized to the quantum yield of Trp-57 (W158S) at pH 7.5, which is considered to be 1. Yields were determined from the total integrated area of the emission curves from 320 nm to 450 nm, and normalized to ODs at 295 nm. Errors represent standard error for four determinations.

The γ-glutamylphosphate–ADP complex

Isotope exchange experiments have indicated a preferred-ordered mechanism with ATP binding first, followed by glutamate, and then ammonium ion (Meek & Villafranca, 1980; Clark & Villafranca, 1985). The substrate glutamate has also been reported to produce an increase in the intrinsic tryptophan fluorescence of GS (Timmons et al., 1974). This change is negligible when glutamate is added to the substrate-free protein but is detectable when added to the ATP complex of GS. Furthermore, the magnitude of this effect on the fluorescence intensity is highly dependent on pH and metal. Mg^{2+}-GS exhibits a much larger increase in steady-state fluorescence when glutamate is added to the ATP complex, than the Mn^{2+} enzyme. The steady-state increase in intensity of Mn^{2+}-GS at pH 6.5 is only 5–8% when glutamate is added to the ATP complex. However, all of the fluorescence characterization using phase/modulation experiments to date have been with the Mn^{2+} enzyme. Therefore, we have also investigated the fluorescence changes accompanying glutamate binding to the ATP complex for the Mn^{2+}-GS. Even though the steady-state fluorescence intensity change induced by glutamate is small, detailed analysis of the lifetime distribution indicates a significant change in the decay parameters associated with Trp-158. Results from global analysis utilizing phase and modulation data for the ATP–GS complex and the glutamylphosphate–GS complex of the wild-type GS are summarized in Table 2 (see also Kinemages 4–6). Pre-steady-state binding studies with ATP (Abell & Villafranca, 1991) have been performed, and it is documented that the Glu–ATP–GS complex quickly reacts to form the γ-glutamylphosphate–ADP complex, which in turn slowly reacts to afford the cyclic pyrrolidone. The formation of γ-glutamylphosphate does not require NH_4^+ (Clark & Villafranca, 1985). In order to minimize time-dependent changes in the nature of the complex during data acquisition, new samples were prepared for each emission wavelength. Typically, 30 min are required to acquire phase and modulation data at 12 modulation frequencies for each wavelength. The previous isotope exchange and rapid quench experiments indicate that in the absence of NH_4^+, the γ-glutamylphosphate intermediate forms within seconds and is very "sticky" with respect to dissociation from the enzyme (Meek et al., 1982; Clark & Villafranca, 1985). Presumably, the cyclization reaction that yields pyrrolidone carboxylate takes place in solution rather than within the enzyme active site

Table 2. *Global analysis for ATP and ADP-glutamylphosphate complexes*[a]

Protein	Ligand	χ^2	Lifetimes (ns)	Fraction intensity, 320, 330, 360, 380 nm
Wild type		1.75	5.23	0.31, 0.33, 0.36, 0.40
			+0.70/−0.47	
			2.49	0.60, 0.60, 0.59, 0.56
			+0.41/−0.89	
			0.61	0.09, 0.07, 0.05, 0.04
	+ATP		5.23	0.85, 0.83, 0.83, 0.82
			2.49	0.13, 0.13, 0.14
			0.61	0.04, 0.03, 0.03
	+ATP		8.69	0.22, 0.25, 0.20, 0.27
	+Glu		+0.98/−0.42	
			4.08	0.72, 0.68, 0.72, 0.64
			+0.59/−0.38	
			0.89	0.06, 0.07, 0.07, 0.09
W57L		1.61	5.67	0.37, 0.39, 0.43, 0.49
			+0.17/−0.31	
			2.35	0.58, 0.56, 0.54, 0.48
			+0.70/−0.45	
			0.35	0.05, 0.05, 0.04, 0.03
	+ATP		5.67	0.73, 0.78, 0.76, 0.74
			2.45	0.25, 0.20, 0.22, 0.24
			0.35	0.02, 0.02, 0.02, 0.02
	+ATP		6.91	0.41, 0.48, 0.44, 0.41
	+Glu		+1.05/−0.85	
			3.61	
			+0.89/−1.13	0.55, 0.45, 0.49, 0.50
			0.80	0.04, 0.07, 0.06, 0.09
W158S		1.65	5.29	0.49, 0.53, 0.59, 0.64
			+0.37/−0.29	
			2.19	0.47, 0.44, 0.39, 0.33
			+0.41/−0.36	
			0.14	0.04, 0.03, 0.03, 0.02
			+0.09/−0.15	
	+ATP		5.29	0.91, 0.89, 0.89, 0.83
			2.19	0.08, 0.09, 0.09, 0.02
			0.14	0.01, 0.02, 0.02, 0.05
	+ATP		5.42	0.90, 0.86, 0.84, 0.79
	+Glu		1.95	0.08, 0.10, 0.13, 0.18
			0.12	0.02, 0.04, 0.03, 0.03

[a] Errors reported for the lifetime values represent the high and low limits of resolution at the 67% confidence level. These limits are obtained from rigorous error analysis as provided by Globals Unlimited. Measurements were made with 10-20 μM protein in 20 mM Hepes, pH 6.5, 100 mM KCl, 1 mM $MnCl_2$ at 20 °C. Final concentrations of ATP and glutamate were 800 μM and 1 mM, respectively. Modulation frequencies were the same as in Table 1.

(Tsuda et al., 1972). Therefore, in the presence of saturating ATP and glutamate, it is likely that a complex equilibrium exists, where a fraction of γ-glutamylphosphate and ADP may dissociate from the enzyme, but free enzyme would rapidly react with free substrates to regenerate this intermediate. Only after depletion of substrates would the population of enzyme complexes become heterogeneous. The observation that changes in fluorescence data occurred after 30 min may indicate that cyclization of the intermediate was taking place and that glutamate and ATP were becoming depleted.

With the wild-type GS, addition of glutamate to the ATP complex causes no dramatic shift in the phase and modulation curves, as is observed with ATP binding. However, it is clear from the global analysis that the recovered lifetime values or their fractional intensities have changed. When all the phase and modulation data for the protein in the absence of ligands, in the presence of ATP, and with glutamate are included in a single global analysis, and the lifetime values are allowed to vary with the different ligand states, the χ^2 value is 1.81 and the recovered lifetimes are very near 5 ns, 2.3 ns, and 0.3 ns for the ligand-free and ATP-bound states of the protein. The fractional intensities change as indicated previously to afford a preponderance of the long lifetime component when ATP is present. Comparison of these two ligand states affords lifetime values that differ by less than 0.4 ns. However, the phase/modulation data associated with glutamate addition afford lifetime values of 8.72 ns (28-30%), 3.87 ns (63-66%), and 0.81 ns (2-7%). Based on the previous results and the data included here, ATP binding is best described by a model where the lifetimes do not change upon addition of ATP, but their relative distribution does. Therefore, we have performed a combined global analysis on the glutamylphosphate-ADP-GS complex with the substrate-free and ATP-complexed enzyme, using a linkage scheme where the lifetime values were constrained to remain the same for these two ligand states and the lifetime components associated with the glutamylphosphate-ADP-GS complex were allowed to vary independently. The χ^2 value for this global analysis is 1.75. The recovered lifetime values for the substrate-free and ATP-bound enzyme are 5.23 ns, 2.49 ns, and 0.61 ns and the fractional intensities change in a manner analogous to the previous observations. In contrast however, the lifetime values associated with the glutamate complex remain higher, 8.69 ns (23-27%), 4.08 ns (64-72), and 0.89 ns (6-9%). When the lifetime components are constrained to remain the same for all three ligand states, the χ^2 value increases significantly to 3.15. The recovered lifetimes are 5.95 ns, 2.79 ns, and 0.68 ns. In this global analysis the fractional intensities change as expected for the ATP complex, but when glutamate is added the fractional intensities change by only 2-3% compared to the ATP complex. This result is inconsistent with the observation that the steady-state fluorescence intensity increases when glutamate is added. Therefore, it appears that glutamate addition to the ATP complex results in a complex with fluorescence lifetimes that differ from those found in the ATP complex. These results are summarized in Table 2. It must be pointed out that the global analysis used here has not been expanded to accommodate more complicated decay schemes with more than three components. It is likely that the two tryptophans are affected independently by addition of gluta-

mate and that there may be more than three individual components in the glutamylphosphate-ADP complex of the wild-type protein. Therefore, analysis of the single tryptophan mutants is expected to be more informative, and the analysis of the wild-type protein should be used as a point of reference. When the phase and modulation data obtained for the W57L mutant are analyzed by comparing similar linkage schemes, Trp-158 demonstrates a similar change in the recovered lifetime values when glutamate is added to the ATP complex.

When the phase and modulation data for the substrate-free, ATP-GS, and glutamylphosphate-ADP complexes of the W57L mutant are combined into a single global analysis and the individual lifetime values are constrained to remain the same for all ligand states, the χ^2 value is 2.25 and the recovered lifetimes are 5.82 ns, 2.45 ns, and 0.45 ns. For the ligand-free data set, the fractional intensities are 34–45% for the long lifetime component, 50–59% for the median lifetime component, and 4–7% for the short-lived component. The fractional intensities change to 70–77%, 21–27%, and 1–3% for the long, the median, and the short components, respectively, when ATP is added. With the subsequent addition of glutamate, this linkage scheme affords fractional intensities of 67–74% for the long lifetime component, 22–29% for the median component, and 1.6–4% for the short component. These fractional intensities are essentially identical to those observed for the ATP complex, prior to addition of glutamate. Based on the observation that the steady-state fluorescence intensity increases 5–8% with glutamate addition, this model does not adequately describe the lifetime distribution of the glutamylphosphate-ADP-GS complex. When a different linkage scheme is used, with the lifetime values constrained to remain the same for the substrate-free and ATP complex, but the lifetimes are allowed to vary for the glutamylphosphate-ADP-GS complex, then the χ^2 value improves to 1.61, and significantly longer lifetimes are observed for this ternary complex. Specifically, the recovered lifetime values for this species are 6.91 ns, 3.61 ns, and 0.80 ns. The fractional intensities are 41–48% for the long component, 49–55% for the median lifetime, and 4–9% for the short lifetime. This is similar to the situation observed for the wild type, although the shift in lifetimes is not as dramatic. Rigorous error analysis of the recovered lifetimes indicates that the long lifetime in the absence of glutamate is well resolved on both sides of the confidence plot, 5.67 ns +0.17/−0.31 for the 67% interval. For the glutamylphosphate-ADP complex the long lifetime is well resolved on the short side but poorly resolved on the longer side, 6.91 ns +1.05/−0.75. The long lifetime values obtained for the presence and absence of glutamate are not as well resolved as they are for the wild type, but the relative changes in recovered lifetime values appear to be nearly identical for these two proteins. As with the long lifetime component, error analysis on the median component indicates that it is also not as well resolved in the glutamylphosphate-ADP complex, 3.61 ns +0.89/−1.13. However, when compared to the data obtained with the wild type, it is reasonable to propose that addition of glutamate affords species with lifetime values that are different from the ATP complex, and that these new species may result from changes induced at Trp-158. These results are summarized in Table 2. In contrast to the results observed with Trp-158, Trp-57 is relatively unaffected when glutamate is added to the ATP complex.

Addition of saturating levels of glutamate to the ATP-W158S complex produces a negligible increase in the steady-state fluorescence. Phase/modulation experiments for the glutamylphosphate-ADP-W158S species suggest no detectable change in the recovered lifetimes or their relative fractional intensities. When the phase and modulation data are analyzed with a linkage scheme in which the lifetimes are constrained to remain the same for all three ligand states, the χ^2 value is 1.85 and the recovered lifetimes are 5.40 ns, 2.25 ns, and 0.21 ns. The fractional intensities change to afford approximately 90% of the long lifetime when ATP is added, as described previously. For the glutamylphosphate-ADP complex, the fractional intensities remain nearly identical except that the median component increases from 10–16% to 9–19% at the expense of the short component. When an alternative linkage scheme is utilized in which the lifetimes are constrained to remain the same for the substrate-free and ATP complex, but are allowed to vary for the glutamylphosphate-ADP complex, the χ^2 value decreases slightly to 1.65. The recovered lifetime values for the substrate-free and ATP complex are 5.29 ns, 2.19 ns, and 0.14 ns. For the glutamylphosphate-ADP complex, the lifetimes are 5.42 ns, 1.95 ns, and 0.12 ns with fractional intensities of 79–90%, 9–18%, and 1.5–3.5% for the long, the median, and the short components, respectively. When rigorous error analysis is performed, the lifetime values recovered for the glutamylphosphate-ADP complex are not resolved from the ATP complex and substrate-free species. Thus, it appears that the effects of glutamate observed with the wild-type protein are nearly completely accounted for by changes at Trp-158, although there may be a small increase in the fractional intensity of the median component of Trp-57. These results are compared in the fractional intensity plots (SAS) shown in Figure 2 and Table 2. It is noteworthy that the wild type is mimicked so closely by the W57L mutant with regard to addition of glutamate. It would be expected that the wild type should possess the individual components contributed by both Trp-57 and Trp-158, and therefore there should be components corresponding to approximately 5 ns and 2.5 ns in the glutamylphosphate-ADP complex of the wild type. It must be pointed out that the analysis is forced to fit the data to a three-component model. The global analysis used does not readily accommodate more complex models involving five or six lifetimes. Because

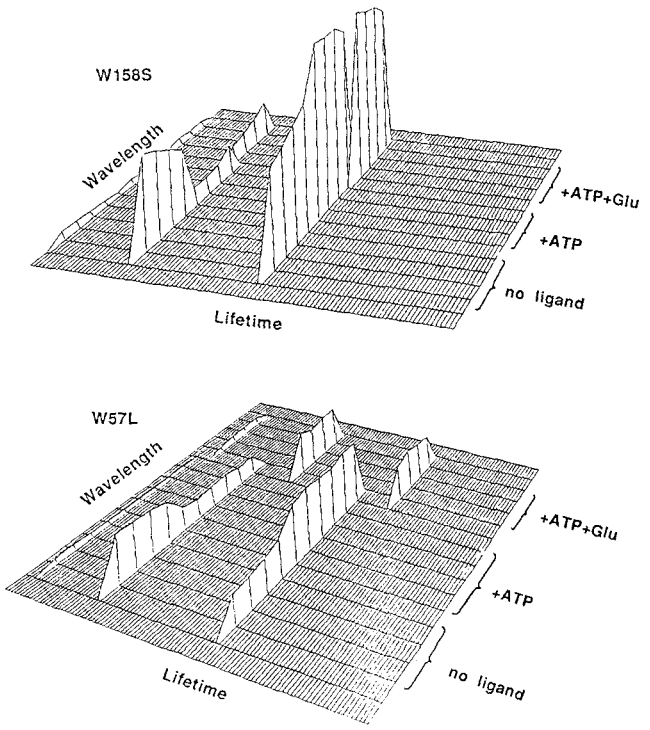

Fig. 2. SAS (species-associated spectra) plots for Trp-57 and Trp-158 in three ligand states. The first four channels along the wavelength axis represent emission intensities for the lifetime components at 320, 330, 360, and 380 nm in the absence of substrate. For the W158S mutant the second four channels, moving back, represent the intensities of the lifetime components at these wavelengths for the ATP-bound protein. For the W57L mutant there are six channels corresponding to the ATP complex. The last four channels represent the intensities for the glutamylphosphate-ADP complex. The lifetime values for the substrate-free and ATP-complexed proteins have been constrained to be the same. The vertical axis, upward from the wavelength-lifetime plane, is normalized to 1 for each of the models shown, so intensities do not reflect relative intensities of W57L vs. W158S. The lifetime values corresponding to these models are shown in Table 2.

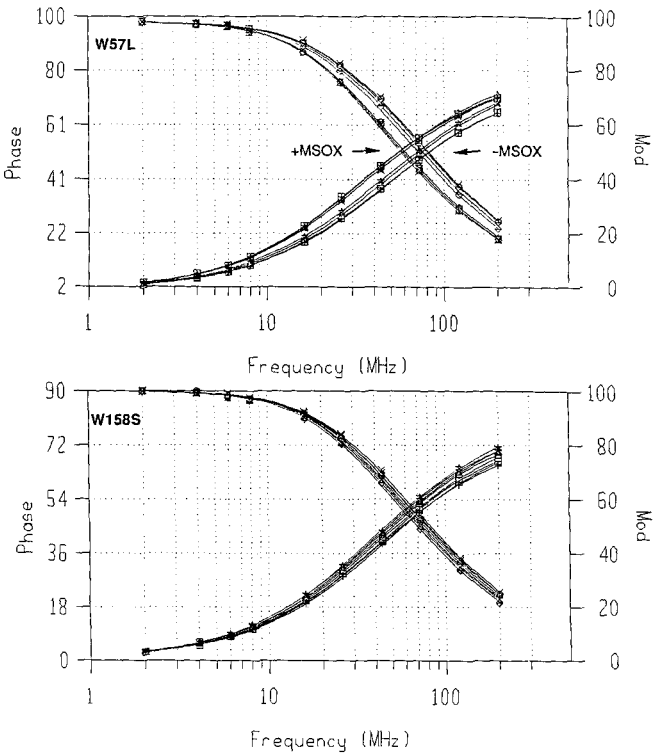

Fig. 3. Phase and modulation data for mutant proteins in the presence and absence of MSOX. Phase angles and modulation ratios were determined at four wavelengths spanning the emission, utilizing 12 modulation frequencies of exciting light (295 nm). The W57L mutant and the wild type demonstrate a marked shift in the frequency response when MSOX is added. W158S demonstrates no effect due to MSOX.

the data have been forced to fit a three-component model, it is likely that the 5-ns component of the Trp-57 collapses with the median component of Trp-158 to afford a median component that is even longer than found for the individual Trp-158. Similarly, the median component of Trp-57 may have collapsed with the short component of Trp-158 to afford a longer component than is actually contributed by Trp-158. Such a simplification of wild-type enzyme decay patterns compared to single-tryptophan-containing mutants has been observed with the lac repressor, where the wild-type protein consists of linear combinations of decay parameters from the individual tryptophans (Royer et al., 1990).

MSOX binding

MSOX mimics the tetrahedral transition state expected for attack of ammonia on the activated γ-glutamylphosphate intermediate formed during catalysis (Manning et al., 1969; Rowe et al., 1969; Eads et al., 1988). It is also established that MSOX interacts with at least one of the active-site metals, presumably the metal at the n_1 site (Eads et al., 1988). Therefore, it is of interest to characterize the structural changes induced by MSOX. Addition of 0.5 mM MSOX to the W57L mutant and the wild-type protein produces a large increase in the steady-state fluorescence intensity (1.4-fold, not shown) as well as a clear shift toward lower modulation frequencies in the phase and modulation data (Fig. 3). It was necessary to determine whether this shift in the frequency response corresponds to a change in the actual recovered lifetime values or whether it reflects a redistribution of existing lifetime components, as described for ATP binding (Atkins et al., 1991).

When the phase and modulation data from the substrate-free W57L protein are included with the data for the MSOX-bound protein, and a combined global analysis is performed with all the lifetimes linked to remain the same in the different ligand states, the χ^2 value is 1.04. When the lifetimes are not linked and allowed to vary between the ligand states, the χ^2 value actually increases slightly to 1.06, and the recovered lifetimes are

nearly identical to those recovered when the lifetime values are constrained to remain the same. Thus, it seems that MSOX causes a redistribution of the existing lifetimes of Trp-158, without resulting in the existence of new lifetimes associated with new microconformational states. These results are summarized in Table 3 and are very similar to what is observed with the wild-type protein. With the wild-type enzyme, however, the data are nearly equally consistent with a model in which the existing lifetimes redistribute and one in which new lifetimes are present, possibly indicating the existence of new microconformational states resulting from the addition of this inhibitor. Still, we have chosen to include the results of the analysis in which all the lifetimes are linked across ligand states for wild-type GS in Table 3. When the lifetime values in the presence of MSOX are allowed to vary independently from the lifetime values in the absence of MSOX, the χ^2 value decreases slightly suggesting a better fit to the data than the model in which the lifetimes are constrained across ligand states ($\chi^2 = 1.73$). The recovered lifetime values are 4.49 ns, 1.92 ns, and 0.33 ns in the absence of MSOX and 5.47 ns, 1.90 ns, and 0.35 ns in the presence of MSOX. However, rigorous error analysis shows that the lifetimes are not resolved from each other at the 67% confidence level. Specifically, the associated errors are 4.49 +1.1/−0.32 ns and 5.47 +0.3/−0.25 ns for the long components. The long lifetimes are poorly resolved on the long side of the confidence plots. Therefore, we have chosen to report the results utilizing the model in which the three lifetimes are constrained to remain the same in the presence and absence of MSOX.

Table 3. *Combined global analysis for wild type and Mutants ±MSOX*[a]

Protein	Ligand	χ^2	Lifetime (ns)	Fraction intensity, 320, 330, 360, 380 nm
Wild type	−MSOX	1.73	5.79 +0.29/−0.21	0.23, 0.25, 0.27, 0.30
			2.72 +0.30/−0.22	0.65, 0.65, 0.66, 0.64
			0.75 +0.20/−0.21	0.12, 0.10, 0.07, 0.06
	+MSOX		5.79 +0.29/−0.21	0.70, 0.72, 0.66, 0.61
			2.72 +0.30/−0.22	0.25, 0.24, 0.31, 0.35
			0.75 +0.20/−0.21	0.05, 0.04, 0.03, 0.04
W57L	−MSOX	1.04	5.89 +0.11/−0.15	0.34, 0.37, 0.40, 0.46
			2.39 +0.13/−0.12	0.60, 0.58, 0.56, 0.51
			0.35 +0.13/−0.16	0.06, 0.06, 0.04, 0.03
	+MSOX		5.89 +0.11/−0.15	0.67, 0.67, 0.65, 0.62
			2.39 +0.13/−0.12	0.30, 0.30, 0.33, 0.35
			0.35 +0.11/−0.16	0.03, 0.03, 0.03, 0.03
W158S	−MSOX	1.09	5.25 +1.2/−0.33	0.52, 0.56, 0.62, 0.68
			2.09 +0.60/−0.18	0.42, 0.40, 0.35, 0.30
			0.19 +0.70/−0.54	0.04, 0.03, 0.03, 0.02
	+MSOX		5.25 +1.2/−0.33	0.55, 0.60, 0.64, 0.69
			2.09 +0.60/−0.18	0.42, 0.37, 0.34, 0.30
			0.19 +0.70/−0.54	0.04, 0.03, 0.02, 0.02

[a] Errors reported for the lifetime values represent the high and low limits of resolution at the 67% confidence level. These limits are obtained from rigorous error analysis as provided by Globals Unlimited. Measurements were made with 20 μM protein in 20 mM Hepes, pH 6.5, 100 mM KCl, 1 mM $MnCl_2$ at 20 °C. Final concentration of MSOX was 300 μM.

Trp-57, found in W158S and W158F, is much less affected by addition of MSOX. A small increase in fluorescence intensity is observed in the steady-state spectrum (9% increase in peak intensity), but the phase and modulation data for the W158S mutant in the presence and absence of MSOX are nearly superimposable (Fig. 3). Phase and modulation experiments have not been performed with the W158F mutant, but the steady-state spectrum of this mutant is only affected very slightly by addition of MSOX. In addition time-domain experiments with the W158F protein indicate that MSOX has essentially no effect on the recovered lifetime values or on the fractional contribution of the individual decay components (not shown). Global analysis for the W57L mutant utilizing data in the presence and absence of MSOX yields variable results depending on the linkage scheme. The situation is similar to that observed with the wild-type protein. When all the lifetimes are constrained to remain the same in the presence and absence of MSOX, the χ^2 value increases to 1.93, compared to 1.04 when the lifetimes are allowed to vary between ligand states. However, error analysis for the model in which the lifetimes vary indicates that the recovered lifetime components are not resolved from one another. It is possible that the wild type and Trp-158 mutant possess lifetime components when MSOX is present that are not evident in the absence of MSOX, particularly for the longest components, but within the resolution of our data we cannot distinguish where the recovered lifetimes actually differ for the two ligand states. Therefore, we have considered the effects as reflecting a change in the fractional intensities only. For W158S this change is only a few percent. Thus, it appears that although there is a small change in the fluorescence parameters of Trp-57 when MSOX binds, there is a much larger perturbation at Trp-158. MSOX results in a larger proportion of the long lifetime for Trp-158. It is essential to note that MSOX does bind to W158S and

W158F mutants. A number of observations support this: (1) W158S is inhibited by comparable concentrations of MSOX as the wild type in the standard γ-glutamyl transferase assay (data not shown). (2) In addition, the W158F mutant is inhibited by MSOX and exhibits a K_m for glutamate that is nearly identical to the wild-type protein, indicating that the glutamate-binding pocket is unperturbed. This W158F mutant also demonstrates only a minor (10%) increase in the steady-state fluorescence intensity when MSOX is added. (3) MSOX produces a dramatic increase in the steady-state fluorescence intensity of the wild type, the W158F mutant, and the W158S mutant, suggesting that the binding of this transition-state analogue is not affected by mutations at Trp-158. It is not likely that MSOX-P would bind tightly to these mutants and MSOX would not. Addition of the phosphate moiety to the MSOX structure is sufficient to recruit the Trp-57 loop toward the active site, as is seen when ATP is added. Notably, the magnitude of the fluorescence change observed with MSOX-P is smaller than with ATP, and when ADP is added to the MSOX-P complex of the wild-type, W158S, and W158F proteins, an additional increase in fluorescence intensity is observed. (4) As noted above, the W158S mutant does not demonstrate a large difference in the K_m for glutamate in either the Mn- or the Mg-dependent biosynthetic assay. For both forms of the enzyme there is an approximate twofold increase in the K_m for this substrate. It is noteworthy that the relative magnitude of the change in fractional intensities of the individual lifetime components is larger for the wild-type enzyme than either of the mutants when MSOX is added. It is possible that the magnitude of the shift in the equilibrium between microconformational states that is caused by MSOX is not as large for the mutant protein as it is for wild-type GS.

The inactivated ADP-MSOX-P complex

The inactivated complex obtained by addition of MSOX and ATP was also examined by phase and modulation measurements. The inactive complex results from phosphoryl transfer to MSOX to produce tightly bound MSOX-P and ADP. This complex closely mimics the tetrahedral transition state expected for nucleophilic attack of ammonia that occurs in the ternary complex, ADP-γ-glutamylphosphate-NH_3. Time-resolved fluorescence analysis of this complex provides information about the dynamics of the tryptophan residues in true chemical transition states.

Phase angles and modulation ratios are measured after addition of ATP to samples containing MSOX. For the wild-type and W158S proteins, there is a 1.5–1.6-fold increase in the steady-state fluorescence when ATP is added. For W57L there is a small 1.2-fold increase in intensity, after the large increase resulting from MSOX. Several global analysis models in which lifetime values were constrained to remain the same after addition of ATP were compared to models in which the lifetime values varied with ligand state. As pointed out above, the wild-type protein is expected to have more than three lifetime components, which are collapsed to the linear combination of three lifetimes in this analysis. The W57L and W158S mutants are more easily interpreted. Global analysis of the W57L mutant affords lifetimes that are very similar to those obtained with the ADP-glutamylphosphate complex. Results from the MSOX-P-ADP complex are shown in Table 4. The most striking result is that the lifetime values are significantly longer after addition of ATP to the MSOX complex. The values change from 5.88 ns, 2.12 ns, and 0.19 ns in the absence of ATP to 6.99 ns, 3.65 ns, and 0.81 ns for the MSOX-P-ADP complex. It is noteworthy that the fractional intensities are nearly evenly distributed between the long and median lifetime components with a minor contribution from the short lifetime. This also is reminiscent of the results obtained with W57L in the γ-glutamylphosphate-ADP complex.

Results for the W158S mutant when the MSOX-P-ADP complex is formed provide two models that appear to fit the data equally well, yet one of these models seems more reasonable in light of several observations. Addition of ATP to the MSOX complex of W158S induces a significant change in the steady-state fluorescence intensity. When global analysis is performed with the lifetime values constrained to be the same in the absence and presence of ATP, the recovered lifetimes (5.52, 2.42, and 0.44 ns) and fractional intensities are nearly identical to those in Table 3. Addition of ATP affords nearly com-

Table 4. *Global analysis for MSOX-ATP complex*[a]

Protein	Ligand	χ^2	Lifetime (ns)	Fraction intensity, 320, 330, 360, 380 nm
W57L	MSOX	2.28	5.89	0.78, 0.73, 0.68, 0.65
			2.12	0.20, 0.24, 0.30, 0.33
			0.19	0.02, 0.02, 0.02, 0.03
	+ATP		6.98	0.39, 0.46, 0.43, 0.52
			3.65	0.56, 0.46, 0.50, 0.52
			0.81	0.05, 0.07, 0.07, 0.09
W158S	MSOX	1.44	5.52	0.46, 0.50, 0.55, 0.59
			2.42	0.48, 0.45, 0.41, 0.38
			0.44	0.06, 0.05, 0.04, 0.04
	+ATP		5.52	0.96, 0.98, 0.97, 0.95
			2.42	0.03, 0.00, 0.01, 0.03
			0.44	0.02, 0.02, 0.02, 0.03
W158S	MSOX/+ATP	1.25	8.19	0.14, 0.16, 0.19, 0.22
			5.04	0.85, 0.83, 0.79, 0.74
			0.25	0.01, 0.01, 0.02, 0.04

[a] Measurements were made with 10 μM protein in 20 mM Hepes, pH 6.5, 100 mM KCl, 1 mM $MnCl_2$ at 20 °C. Final concentrations of ATP and MSOX were 800 μM and 100 μM, respectively. Modulation frequencies were the same as Table 1.

plete intensity from the long lifetime component, 95–98%. Only 1–2% of the fractional intensity is associated with the 2.42-ns and 0.44-ns components. The χ^2 for this global analysis is 1.44. When the lifetimes are allowed to vary between the MSOX complex and the MSOX-P-ADP complex, a significant difference in lifetimes is seen for the two states of the protein. The lifetime components for the MSOX-P-ADP complex are 8.19 ns, 5.03 ns, and 0.25 ns with fractional intensities of 13–22%, 75–85%, and 1–3%, respectively. The lifetime values and fractional intensities prior to addition of ATP are essentially the same as those when the lifetime values are fixed for the two ligand states, above. The χ^2 value for this analysis is 1.44. The slight increase in χ^2 for the increased number of linkages makes it impossible to distinguish which of these models fits the data more accurately. These two models are also presented in Table 4. A few observations lead us to conclude that the first of these models is more acceptable. When rigorous error analysis is performed on the model, which allows the lifetimes to vary in the MSOX-P-ADP complex, the recovered lifetimes are not well resolved from one another. At the 67% confidence level, the long lifetime (8.19 ns) in the MSOX-P-ADP complex may be as low as 5.99 ns, and the median lifetime (5.03 ns) is only resolved to values between 3.86 and 5.66 ns. Thus, rigorous error analysis suggests that, at the 67% confidence level, the lifetime values associated with the MSOX complex and the MSOX-P-ADP complex are not resolved. Also, examination of the phase and modulation data suggests that the first model presented in Table 4 is more accurate. Whereas nearly all of the complexes discussed here and in the previous work (Atkins et al., 1991) show small wavelength dependencies across the emission spectrum, there is essentially no wavelength dependence in the MSOX-P-ADP complex of the W158S mutant. Sources of wavelength dependence include ground-state heterogeneity where the individual components have different emission spectra, and dipolar or solvent relaxations that occur on the time scale of emission. For essentially all of the complexes that show wavelength dependence, global analysis yields a model with significant contributions from the long and median lifetime components. The Trp-57 emission of the ATP complex demonstrates very little wavelength dependence and fits best to a model with nearly homogeneous decay. The MSOX-P-ADP species shows even less wavelength dependence in the phase and modulation data, suggesting an even more homogeneous population of the Trp-57 residues. To the extent that this complete lack of wavelength dependence suggests homogeneous decay, the second model for the W158S-MSOX-P-ADP complex (Table 4) is less appealing. Additional experiments with time-resolved anisotropy are needed to completely resolve the two possible models shown in Table 4. The SAS for the MSOX and MSOX-P complexes of the individual tryptophans are shown in Figure 4.

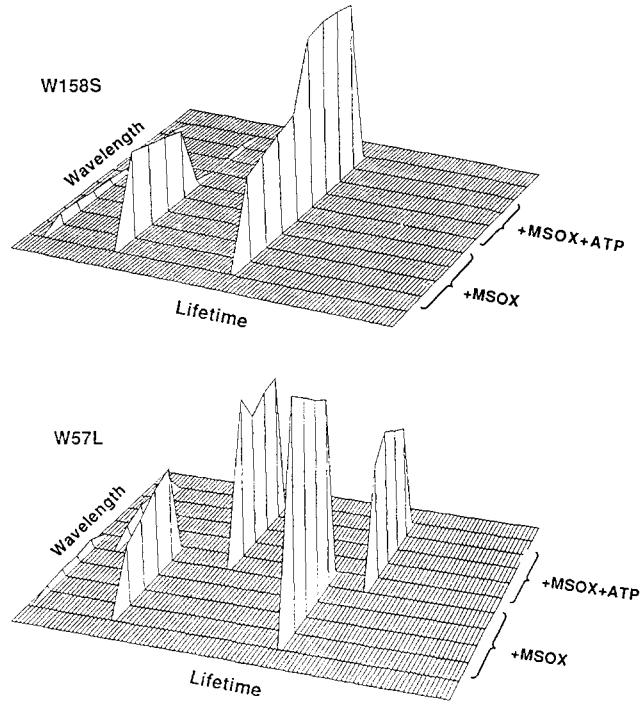

Fig. 4. SAS for the MSOX and MSOX-ATP complexes of mutant proteins. The first four channels along the wavelength axis represent the fractional intensities of the individual lifetime components at four wavelengths in the presence of MSOX. The second four channels represent the fractional intensities in the presence of MSOX and ATP. The vertical axis is normalized to 1 in each individual model and does not reflect the relative intensities of W158S vs. W57L. At some of the channels along the wavelength axis that correspond to different ligand states, there appears to be overlap of two or more lifetime components. This is an artifact of the software, which connects the first and last emission intensity of a ligand state to zero intensity in the channel adjacent to it.

Discussion

The effects of the substrates ATP and glutamate, and of the transition-state analogue MSOX, on the fluorescence decay kinetics of Trp-57 and Trp-158 of *E. coli* glutamine synthetase have been determined with single tryptophan-containing site-directed mutants. The studies presented here utilize the Mn-enzyme at pH 6.5, in contrast to the previous work, which characterized the substrate-free and ATP-bound enzyme at pH 7.4. The extension of the previous work to lower pHs was prompted by the observation that the magnitudes of the steady-state fluorescence changes are typically larger at pH 6.5 than pH 7.4 for the Mn-enzyme. In addition, the Mn-enzyme is optimally active near pH 6.5 and less active at pH 7.5 (Ginsburg et al., 1970).

Here it is demonstrated that at pH 6.5 the lifetime values recovered for each tryptophan are essentially identical to those at pH 7.4. As was observed at pH 7.4, both tryptophans are best described as the sum of three discrete exponentials. Attempts to fit the phase and modu-

lation data to single exponentials or the sum of two discrete components result in significant increases in the χ^2 values. Similarly, fitting to several models that treat the data as continuous distributions of lifetimes results in elevated χ^2 values. There appears to be a small pH dependence to the fractional intensities of the lifetimes associated with Trp-57. At pH 6.5 the long lifetime is not as dominant as it is at pH 7.4, changing from 65% at the higher pH to 50% at pH 6.5.

An additional difference that exists at the different pHs is the relative sensitivity of Trp-158 to the substrate ATP. It was demonstrated previously that Trp-158 was only slightly affected by the addition of ATP at pH 7.4, whereas Trp-57 undergoes a dramatic change in the relative contribution of the individual lifetime components. At pH 6.5, however, Trp-158 also undergoes an apparent redistribution of lifetime components, which is analogous to, but not as large as, the effect observed with Trp-57. This can be attributed to an increase in the relative quantum yield of Trp-158 in the ATP complex as the pH is lowered from 7.5 to 6.5. The quantum yield of either tryptophan for the substrate-free enzyme is relatively insensitive to pH over the range from 6.5 to 7.5. At the lower pH, Trp-158 demonstrates a shift in the phase and modulation data to lower frequencies when ATP is added to the enzyme. Global analysis suggests that this corresponds to a redistribution of the existing lifetime components rather than a structural change that results in the presence of new lifetime components. Although it is possible that both tryptophans actually adopt new conformations when ATP binds, the previous work and the results presented here suggest that there is instead a general "tightening" of the relatively dynamic GS molecule. We propose that both the central loop and the Trp-57 loop sample several microconformational states that are in thermal equilibrium, and binding of the substrate ATP alters the microconformational equilibrium in both regions of the protein. The two regions of the protein differ markedly, however, in the relative degree of heterogeneity of the local microconformational distribution. Whereas Trp-57 becomes almost completely "locked" into a single conformation (90%), Trp-158 remains significantly more heterogeneous, and no single lifetime component completely dominates when ATP is bound. It is noteworthy that Trp-158 undergoes this redistribution to a much larger extent at pH 6.5 than at pH 7.4. It is reasonable to speculate that the pH profile of the Mn-enzyme may be linked to the ability of the enzyme to effectively redistribute these microconformations when ATP binds. In contrast to our previous observation that the substrate ATP causes a localized effect on GS dynamics at pH 7.4, ATP has a more global effect on the protein at the pH optimum of the Mn-enzyme.

Because the kinetic mechanism of GS is a preferred-ordered mechanism with ATP binding preceding glutamate binding (Meek & Villafranca, 1980; Meek et al., 1982; Clark & Villafranca, 1985), we have also characterized the fluorescence decay kinetics of the complex obtained after addition of glutamate to the ATP complex. This is expected to produce the ADP-glutamylphosphate complex. In marked contrast to the results observed with ATP, addition of glutamate produces an apparent structural change associated with new lifetime components for Trp-158. Specifically, the recovered lifetimes change from approximately 5.5 ns, 2.5 ns, and 0.4 ns to 7 ns, 3.6 ns, and 0.5 ns. Trp-57 is not affected by addition of glutamate to the ATP complex, based on the results obtained with the W158S and W158F mutants. It is noteworthy that the glutamylphosphate–ADP complex still exhibits heterogeneous decay kinetics, suggesting that even during intermediate stages of catalysis the enzyme exhibits microconformational heterogeneity. The conclusion that new lifetimes are produced upon addition of glutamate is supported by the results obtained with the wild-type enzyme. Although we have not expanded the global analysis to accommodate the five or six individual components that might be expected from the two tryptophans in this complex, it is clear that a lifetime significantly longer than 5 ns is present, and, based on the results obtained with the W57L mutant, this is due to a change in lifetime components of Trp-158. We presume, because our analysis limits the wild-type data to the sum of only three exponentials, that several components are collapsed into the median and short lifetimes recovered for the wild-type–ADP–glutamylphosphate complex. Similar interpretation has been offered for the binding of substrates to the lac repressor (Royer et al., 1990) where each of the individual lifetime components found for two different tryptophans was not uniquely recovered with the wild-type enzyme. Although we have not determined the effects of these substrates on the decay kinetics of the Mg form of GS, steady-state experiments at pH 7.4 indicate similar changes, i.e., Trp-57 exhibits a dramatic increase in fluorescence intensity when ATP is added and Trp-158 is affected to a lesser degree. Addition of glutamate results in a small increase in intensity at Trp-158 only. Therefore, we propose that during enzyme turnover for the Mn-enzyme at pH 6.5 or the Mg-enzyme at pH 7.5, there is a global change in the dynamic nature of GS when ATP binds, although the effect is more dramatic at the Trp-57 loop than at the central loop. Upon binding of glutamate, there is a localized conformational change of a region of the protein including Trp-158. This change, in contrast to that produced by ATP, actually results in a new structure in this region of the protein, as indicated by the recovery of new lifetime components.

The results presented here and previously (Atkins et al., 1991) have significant implications for the role of protein dynamics in catalytic function of enzymes (Demchenko, 1986). It is noteworthy that binding of the single substrate ATP results in a change from a very heterogeneous distribution of lifetime components to a nearly homoge-

neous system with 90% of the existing lifetime components in one microconformation. This presumably reflects the "tightening" of the region around Trp-57, and to a lesser degree Trp-158, such that the protein is not sampling different microconformations with the same frequency as in the absence of ATP. The results obtained with the glutamylphosphate–ADP complex and the MSOX-P–ADP complex are noteworthy. Whereas the substrate ATP and the "partial" transition-state analogue MSOX do not result in the presence of new lifetime components, transfer of phosphate to glutamate or to MSOX results in a conformational change at Trp-158, which is associated with new lifetime components. Specifically, Trp-158 undergoes a conformational change when these species are generated at the active site, but this region of the protein still exhibits a significant degree of heterogeneity. Trp-57 is very dynamic in the substrate-free enzyme, becomes conformationally locked when ATP is bound, and becomes even more homogeneous as the active site proceeds through phosphorylation of glutamate or MSOX (Fig. 4). Considerable discussion has suggested a role for protein dynamics during chemical events along the reaction pathway of enzymes (Demchenko, 1986) and the fact that enzyme active sites are more flexible than structural elements located far from catalytic residues (DeBrunner & Fraunfelder, 1982). Time-resolved anisotropy measurements and other experimental approaches, which directly monitor molecular motion, may definitively determine whether the heterogeneity associated with Trp-158 in the transition-state complex corresponds to freely mobile residues near the active site. GS appears to provide evidence that enzyme-bound intermediates do not necessarily lead to a completely frozen enzyme in a single, homogeneous microconformational state.

Materials and methods

Site-directed mutagenesis and cell growth

Site-directed mutagenesis was performed according to the method of Kunkel (1985). This was accomplished using single-stranded template obtained from a plasmid constructed by subcloning the EcoRI–HindIII fragment from the previously described pgln6 (Backman et al., 1981) into pTZ18 obtained from Amersham. Template was isolated from *E. coli* strain RZ1032 harboring this construction and coinfected with M13KO7 helper phage. W158F was constructed using an in vitro site-directed mutagenesis kit purchased from Amersham, with non-uracil-containing template DNA. After isolation of mutant clones, W57L was expressed in pgln35 by subcloning the BsuII36–BglII fragment into pgln35. W158S was also expressed in pgln35 after construction by analogous methods. All mutant plasmids were transformed into the *E. coli* strain YMC11, which contains a deletion in chromosomal glutamine synthetase (Backman et al., 1981). Wild-type protein was obtained from an overexpression system consisting of the strain YMC10 harboring the plasmid pgln35.

Protein purification and characterization

Wild-type and mutant GS was purified by the zinc precipitation method previously described (Miller et al., 1974). Several growths of the *E. coli* strain YMC11 harboring W57L mutant under conditions that typically afford GS of low adenylylation state resulted in the isolation of W57L, which had an average adenylylation state of 10 or greater. Thus, in order to study the low adenylylation state of this enzyme, it was necessary to perform in vitro deadenylylation. This was accomplished by treatment of purified W57L with snake venom phosphodiesterase, according to the method described by others (Shapiro et al., 1967). A protease inhibitor cocktail including phenylmethylsulfonylfluoride (10^{-3} M final concentration) and pepstatin A (10^{-7} M) was used to inhibit potential proteolysis resulting from the commercially available snake venom phosphodiesterase (Sigma). After phosphodiesterase treatment, the mutant protein was repurified by zinc precipitation and ammonium sulfate fractionation according to the original purification procedure (Miller et al., 1974). This treatment typically resulted in a decrease in the average adenylylation state from greater than 10 to less than 3. The average state of adenylylation of the wild type was determined by the γ-glutamyl transferase assay as described by Stadtman and Ginsburg (1974). The adenylylation state of mutant proteins was determined by quantitation of inorganic phosphate released from acid hydrolysis.

Enzyme activities were determined by the standard γ-glutamyl transferase assay (Woolfolk et al., 1966) and by the biosynthetic assay as described by Kingdon et al. (1968). Characterization of the mutant proteins is described elsewhere (Atkins et al., 1991).

Fluorescence measurements

Steady-state fluorescence experiments were performed on a Photon Technologies International (PTI) LS-100 fluorescence spectrophotometer. Relative quantum yields of the various proteins were determined by integrating the area under the emission curves from 310 nm to 500 nm, using software provided by PTI. Quantum yield values represent the average of three individual determinations with different samples. The areas were integrated three times and the average value was normalized to OD 295 nm of the same sample. For the quantum yield determinations, all ODs at 295 nm were less than 0.05 in order to avoid all inner filter effects.

Time-resolved fluorescence measurements were performed at the Laboratory for Fluorescence Dynamics, University of Illinois at Urbana-Champaign. The frequency response of the proteins was measured using the

cross-correlation phase and modulation fluorimeter described by Alcala et al. (1987), with a harmonic content of 2-MHz pulses from a mode-locked Nd-YAG laser with the frequency doubled. This was coupled to a cavity dumped dye laser (models 7220 and 702) and to an external frequency doubler. Each of these components was obtained from Coherent Corporation. The excitation wavelength was 295 nm and was set with a birefringent crystal of the dye laser. Phase and modulation data were obtained at 320, 330, 360, and 380 nm with emission bandpass filters (8 nm bandpass). Paraterphenyl in cyclohexane was used as a reference compound to correct for color shifts and instrumental phase delay. This reference has a lifetime of 1.06 ns. The error in the phase angles was less than 0.6 degrees and of the demodulation factors was less than 0.004. Fluorescence measurements were performed in 20 mM Hepes, 100 mM KCl, 1 mM $MnCl_2$, pH 6.5. Protein concentrations ranged from 10 to 20 μM. For addition of ligands, aliquots of neutralized stock solutions were added until no further change in steady-state fluorescence was observed. The total concentration of ligand at that point was then tripled. For ATP this was approximately 800 μM; glutamate, 1 mM; MSOX, 300 μM.

The frequency domain multiwavelength data were analyzed using the global analysis software package, Globals Unlimited (Beecham et al., 1983; Knutson et al., 1983; Beecham & Gratton, 1988). This analysis is based on the theories and algorithms of the Marquardt-Levenburg type with nonlinear least-squares analysis. The global analysis allows for the simultaneous fitting of multiple data sets. For an individual data set, each of the lifetime components present is constrained to remain the same at each emission wavelength. Error analysis of the recovered lifetimes was performed by allowing a lifetime value to vary in an incremental fashion while allowing the remaining parameters to relax to new minima, and calculating the new χ^2. Time-domain lifetime measurements were obtained with a PTI LS-100, single-photon counting time-resolved fluorimeter. Excitation was from a nitrogen flash lamp. At each wavelength 15,000 total counts were obtained, with the sample decay compared to the lamp profile every 2,000 counts. Lamp profile was obtained with a 0.5% glycogen solution.

Acknowledgments

We thank Dr. Cathy Royer for enormously helpful suggestions and for help in performing the lifetime measurements. We are also grateful to Dr. Joseph Beecham for helpful discussions concerning global analysis. The frequency domain time-resolved fluorescence measurements were made at the Laboratory for Fluorescence Dynamics (LFD) at the University of Illinois at Urbana-Champaign (UIUC). The LFD is supported jointly by the Division of Research Resources of the National Institutes of Health (RR03155-01) and UIUC. We also gratefully acknowledge Patrice Dombrowsky for construction of the W158S mutant. W.M.A. is supported by NIH grant GM 13714 and J.J.V. is supported by GM 23529.

References

Abell, L.M. & Villafranca, J.J. (1991). Effect of metal ions and adenylylation state on the internal thermodynamics of phosphoryl transfer in the *Escherichia coli* glutamine synthetase. *Biochemistry 30*, 1413-1418.

Alcala, J.R., Gratton, E., & Prendergast, F.G. (1987). Interpretation of fluorescence decays in proteins using continuous lifetime distributions. *Biophys. J. 51*, 925-936.

Almassy, R.J., Janson, L.A., Hamlin, R., Xuong, N.-H., & Eisenberg, D. (1986). Novel subunit-subunit interactions in *Escherichia coli* glutamine synthetase. *Nature 323*, 304-309.

Atkins, W.M., Stayton, P.S., & Villafranca, J.J. (1991). Time-resolved fluorescence studies of genetically engineered *E. coli* glutamine synthetase: Effects of ATP on the Trp-57 loop. *Biochemistry 30*, 3406-3416.

Backman, K., Chen, Y.-M., & Magasanik, B. (1981). Physical and genetic characterization of the glnA-glnG region of the *Escherichia coli* chromosome. *Proc. Natl. Acad. Sci. USA 78*, 3743-3747.

Beechem, J.M., Knutson, J.R., Ross, J.B., Turner, B.W., & Brand, L. (1983). Global resolution of heterogeneous decay by phase/modulation fluorometry: Mixture and proteins. *Biochemistry 22*, 6054-6058.

Beechem, J.R. & Gratton, E. (1988). Fluorescence spectroscopy data analysis. In *Time Resolved Laser Spectroscopy* (Lackowicz, J., Ed.), p. 70. Proc. SPIE-Int. Soc. Opt. Eng. 909.

Clark, D.D. & Villafranca, J.J. (1985). Isotope exchange enhancement studies of *Escherichia coli* glutamine synthetase. *Biochemistry 24*, 5147.

Colombo, G. & Villafranca, J.J. (1986). Amino acid sequence of *Escherichia coli* glutamine synthetase deduced from the DNA-nucleotide sequence. *J. Biol. Chem. 216*, 10587-10591.

Dantry-Varsat, A., Cohen, G.N., & Stadtman, E.R. (1979). Some properties of *Escherichia coli* glutamine synthetase after limited proteolysis by subtilisin. *J. Biol. Chem. 254*, 3124-3128.

DeBrunner, P.G. & Fraunfelder, H. (1982). Dynamic of proteins. *Annu. Rev. Phys. Chem. 33*, 283-289.

Demchenko, A.P. (1986). Fluorescence analysis of protein dynamics. *Essays Biochem. 22*, 120-156.

Denton, M.D. & Ginsburg, A. (1969). Conformational changes in glutamine synthetase from *Escherichia coli*: The binding of Mn^{2+} in relation to some aspects of enzyme activity. *Biochemistry 8*, 1714-1725.

Eads, C.D., LoBrutto, R., Kumar, A., & Villafranca, J.J. (1988). Identification of non-protein ligands to the metal ions bound to glutamine synthetase. *Biochemistry 27*, 165-170.

Eftnik, M.R. & Wasylewski, Z. (1989). Fluorescent lifetime and solute quenching studies with the single-tryptophan containing protein parvalbumin. *Biochemistry 28*, 382-391.

Ginsburg, A. (1972). Glutamine synthetase of *Escherichia coli*: Some chemical and physical properties. *Adv. Protein Chem. 26*, 1-59.

Ginsburg, A., Yeh, J., Hennig, S.B., & Denton, M.D. (1970). Some effects of adenylylation on the biosynthetic properties of the glutamine synthetase from *Escherichia coli*. *Biochemistry 9*, 633-649.

Hutnik, C.M. & Szabo, A.G. (1989a). Confirmation that multiexponential fluorescence decay behavior of holoazurin originates from conformational heterogeneity. *Biochemistry 28*, 3923-3934.

Hutnik, C.M. & Szabo, A.G. (1989b). A time-resolved fluorescence study of azurin and metalloazurin derivatives. *Biochemistry 28*, 3935-3939.

Janson, C.A., Almassy, R.J., Westbrook, E.M., & Eisenberg, D. (1984). Isolation and crystallization of unadenylated glutamine synthetase from *Salmonella typhimurium*. *Arch. Biochem. Biophys. 228*, 512-518.

Kingdon, H.S., Hubbard, J.S., & Stadtman, E.R. (1968). Regulation of glutamine synthetase XI. The nature and implication of a lag phase in the *E. coli* glutamine synthetase reaction. *Biochemistry 7*, 2136-2142.

Knutson, J.R., Beechem, J.R., & Brand, L. (1983). Simultaneous anal-

ysis of multiple fluorescence decay curves: A global approach. *Chem. Phys. Lett. 102*, 501-507.

Kunkel, T.A. (1985). Rapid and efficient site-specific mutagenesis without phenotypic selection. *Proc. Natl. Acad. Sci. USA 82*, 488-492.

Lackowicz, J.R. (1983). *Principles of Fluorescence Spectroscopy*. Plenum Press, New York.

Manning, J.M., Moore, S., Rowe, W.B., & Meister, A. (1969). Identification of L-methionine S-sulfoximine as the diastereoisomer of L-methionine SR-sulfoximine that inhibits glutamine synthetase. *Biochemistry 8*, 2681-2685.

Maurizi, M.R. & Ginsburg, A. (1982). Active site ligand stabilization of quaternary structure of glutamine synthetase. *J. Biol. Chem. 257*, 7246-7251.

McNemar, L.S., Lin, W-Y., Eads, C.D., Atkins, W.M., Dombrowsky, P., & Villafranca, J.J. (1991). Terbium(III) luminescence study of the spatial relationship of tryptophan residues to the two metal ion binding sites of *Escherichia coli* glutamine synthetase. *Biochemistry 30*, 3417-3421.

Meek, T.D., Johnson, K.A., & Villafranca, J.J. (1982). *Escherichia coli* glutamine synthetase. Determination of rate-limiting steps by rapid-quench and isotope partitioning experiments. *Biochemistry 21*, 2158-2167.

Meek, T.D. & Villafranca, J.J. (1980). Kinetic mechanism of *Escherichia coli* glutamine synthetase. *Biochemistry 19*, 5513-5519.

Miller, R.E., Shelton, E., & Stadtman, E.R. (1974). Zinc-induced paracrystalline aggregation of glutamine synthetase. *Arch. Biochem. Biophys. 163*, 155-168.

Moss, J., Stanley, S.J., & Levine, R.L. (1988). ADP-ribosylation of glutamine synthetase. *FASEB J. 2*, A1045.

Rowe, W.B., Ronzio, R.A., & Meister, A. (1969). Inhibition of glutamine synthetase by methionine sulfoximine phosphate. *Biochemistry 8*, 2674-2680.

Royer, C., Gardner, J., Beecham, J.M., Brochon, J.C., & Mathews, K.S. (1990). Resolution of the intrinsic fluorescence decay kinetics of the two tryptophan residues of *E. coli* lac repressor using genetically engineered single tryptophan mutants. *Biophys. J. 58*, 363-373.

Shapiro, B.M., Kingdon, H.S., & Stadtman, E.R. (1967). Regulation of glutamine synthetase VII. Adenylyl glutamine synthetase: A novel form of the enzyme with altered regulatory and kinetic properties. *Proc. Natl. Acad. Sci. USA 58*, 642-649.

Shrake, A., Fisher, M.T., McFarland, P.J., & Ginsburg, A. (1989). Partial unfolding of dodecameric glutamine synthetase from *Escherichia coli*: Temperature induced reversible transitions of two domains. *Biochemistry 28*, 6281-6290.

Stadtman, E.R. & Ginsburg, A. (1974). The glutamine synthetase of *Escherichia coli*: Structure and control. *The Enzymes X*, 755-807.

Timmons, R.B., Rhee, S.G., Luterman, D.L., & Chock, P.B. (1974). Mechanistic studies of glutamine synthetase from *Escherichia coli*. Fluorometric identification of a reactive intermediate in the biosynthetic reaction. *Biochemistry 13*, 4479-4485.

Tsuda, Y., Stephani, R.A., & Meister, A. (1972). Direct evidence for the formation of an acyl phosphate by glutamine synthetase. *Biochemistry 10*, 3186-3189.

Woolfolk, C.A., Shapiro, B.M., & Stadtman, E.R. (1966). Regulation of glutamine synthetase I. Purification and properties of glutamine synthetase from *Escherichia coli*. *Arch. Biochem. Biophys. 116*, 177-192.

Yamashita, M.M., Almassy, R.J., Janson, C.A., Lasek, D., & Eisenberg, D. (1988). Refined atomic model of glutamine synthetase at 3.5 Å resolution. *J. Biol. Chem. 264*, 17681-17688.